Engineering Structures 123 (2016) 124–140

Contents lists available at ScienceDirect

Engineering Structures

journal homepage: www.elsevier.com/locate/engstruct

Experimental study of sustainable high strength steel flush end plate beam-to-column composite joints with deconstructable bolted shear connectors

Abdolreza Ataei *, Mark A. Bradford, Hamid R. Valipour, Xinpei Liu

Centre for Infrastructure Engineering and Safety, School of Civil and Environmental Engineering, UNSW Australia, Sydney, NSW 2052, Australia

ARTICLE INFO

Article history:
Received 30 October 2015
Revised 16 May 2016
Accepted 23 May 2016
Available online 11 June 2016

Keywords:
Semi-rigid beam-to-column joint
Concrete-filled steel tubular column
Bolted shear connectors
Blind bolting
Deconstructability
High strength steel
Sustainability

ABSTRACT

The design of engineering structures for deconstructability can reduce the energy and cost required for their demolition and for the disposal of their construction waste, and it also enhances the sustainability of a building by allowing for easy dismantling and the reuse or recycling of structural components and construction materials at the end of the service life of the building. In addition, using high performance materials such as high strength steel can improve the sustainability of a structure by providing for higher design stresses and accordingly reducing the self-weight of the structure. This paper describes the results of four full-scale beam-to-column deconstructable composite joints with high strength steel S690 flush end plates. The structural behaviour of the new system in conjunction with application of post-installed friction-grip bolted shear connectors for developing deconstructable composite floors is investigated. The test results show that the proposed composite beam-to-column joints can provide the required strength and ductility according to Eurocode 3 and Eurocode 4 specifications, and that the system can be easily deconstructed at the end of the service life of the structure as a proof of concept.

1. Introduction

Among different construction materials, steel has a great potential to significantly improve the sustainability of the construction industry; steel structures have high strength to weight ratios, they can be erected rapidly and their construction and demolition waste can be minimised by employing prefabricated and deconstructable systems. Moreover, using prefabrication and deconstruction in conjunction with steel frames can drastically facilitate the full recycling and reuse of the construction materials and structural components. Accordingly, over the past decade several attempts have been made to enhance the sustainability of steel structures by either using high-strength durable steels [1–4] or developing prefabricated demountable steel framing systems [5–20]; however, the application of HSS in conjunction with deconstructable frames remains unexplored and this is the main focus of the present study.

The use of high strength steel (HSS) with yield stress in excess of 400 MPa has recently gained popularity in the construction industry owing to its higher yield strength, greater corrosion resistance and higher toughness compared with mild steel. In HSS construction, design stresses can be increased and thickness of plates may be reduced which, in turn, can save on the costs of labour, welding, transportation, erection and fabrication. The cost of the foundation may also be reduced owing to lower self-weight of HSS structures compared to mild steel structures [2]. However, the efficient use of HSS in structural members has been hampered by problems associated with its lower ductility, weldability and fatigue resistance. In particular, the lower ductility of the HSS can potentially affect the structural performance of beam-to-column connections where the steel plates can experience large strains well-beyond the yield strain [3,4]. Girão Coelho and Bijlaard [3] carried out an experimental investigation of moment connections with end plates made from high strength steel of Grades S460, S690 and S960 to provide insight into the non-linear behaviour of these joints and it was concluded that the extrapolation of the design philosophy in the current EC3 provisions, based on the semi-continuous/partially-restrained concept, can provide accurate strength predictions. In addition, it was shown that the HSS end plate connections can provide the rotation demands required for beam-to-column connections of rigid and semi-rigid moment resisting frames.

Apart from its attributes of high-strength and high-performance, design for deconstruction in conjunction with the use of recycled steel can significantly enhance the sustainability of steel structures. In a fully deconstructable steel–concrete composite frame, the beam-to-column connections as well as the floor

* Corresponding author. Tel.: +61 2 93855014; fax: +61 2 93859747.
E-mail address: a.ataei@unsw.edu.au (A. Ataei).

http://dx.doi.org/10.1016/j.engstruct.2016.05.035
0141-0296/

slab to steel beam connections should have the potential to be easily dismantled. Bolted beam-to-column connections with flush or extended end plates can partly provide the ease required for dismantling steel frames, but existing composite steel–concrete floor systems typically take advantage of monolithic construction to ensure adequate performance (*i.e.* near to full composite action) and hence they cannot be easily disassembled and reused at the end of the service life of the structure. Furthermore, the demolition of monolithic concrete–steel composite floors in which the shear studs have been permanently buried in cast *in situ* concrete (or pockets filled with grout), requires much energy and leads to large amounts of construction waste and environmental intrusion. Because of this, there is a need to develop deconstructable steel–concrete composite floors that can be easily dismantled at the end of a structure's service life.

Post-installed Friction-grip Bolted Shear Connectors (PFBSCs) installed through bolt holes placed in precast slabs and predrilled in the top flange of the steel beams is a novel method for developing composite action between precast concrete slabs and steel girders. The composite floors employing PFBSCs can be easily dismantled at the end of their service life, and this in turn can minimise the construction waste associated with the demolition of composite floors and can maximise the possibility for future reuse of the structural components [7–24]. Furthermore, demountable composite floors with precast slabs and prefabricated steel girders can increase the speed, accuracy and quality of construction and reduce the time and environmental impact (*viz.* noise, disruption to traffic and pollution) of the construction.

The first tests on bolted shear connectors appear to date back to the late 60s [7], but surprisingly limited studies have been conducted on the behaviour and application of bolted shear connectors since then [8–24], and most of these studies are related to bolted shear connectors permanently buried in concrete or grout-filled pockets [8–12] with less attention being paid to the potential application of PFBSCs for developing deconstructable steel–concrete composite floors [13–24]. In general, the available test results show that bolted shear connectors exhibit higher load capacity and significantly higher fatigue strength than those of stud shear connectors [8–11]. Moreover, limited experimental studies on bridge decks have demonstrated the adequacy of PFBSCs for strengthening non-composite bridge girders by increasing their stiffness, load carrying capacity and fatigue strength [10,11].

This paper presents the results of static tests conducted on four full-scale Flush End Plate Semi-Rigid (FEPSR) beam-to-column joints made up of Grade S690 HSS in a steel–concrete composite frame that takes advantage of deconstructable PFBSCs and precast "Green Concrete" (GC) slabs associated with reduced ordinary Portland cement content [25]. The main objective is to determine the failure mode and characterise the moment and rotation capacity, moment–rotation relationship and ductility of this new sustainable composite system with high strength steel FEPSR beam-to-column joints. Moreover, the provisions of Eurocode 3 (EC3) [26] and Eurocode 4 (EC4) [27] are employed to investigate the structural performance of the HSS FEPSR joints with deconstructable composite beams and the influence of the type of bolted shear connectors, degree of shear connection and type of columns (open sections and concrete filled steel tubes) on the structural behaviour of the proposed composite joints are investigated.

2. Test specimens

2.1. Specimen design

Four full-scale cruciform beam-to-column joints with flush end plates were designed and constructed according to the provisions of EC3 [26] and EC4 [27] to evaluate the stiffness, ductility, bending moment capacity and rotation capacity of the proposed deconstructable composite joints with HSS flush end plates. The beam-to-column assemblages were symmetric to simulate behaviour of an internal joint in a semi-rigid frame. The specimens were tested under a displacement-controlled vertical load applied at the tip of the beam. A schematic outline of the deconstructable composite beam-to-column joint is shown in Fig. 1. The geometry, dimensions and details of all specimens are illustrated in Figs. 2 and 3 and the details of composite beams and the PFBSCs are given in Table 1.

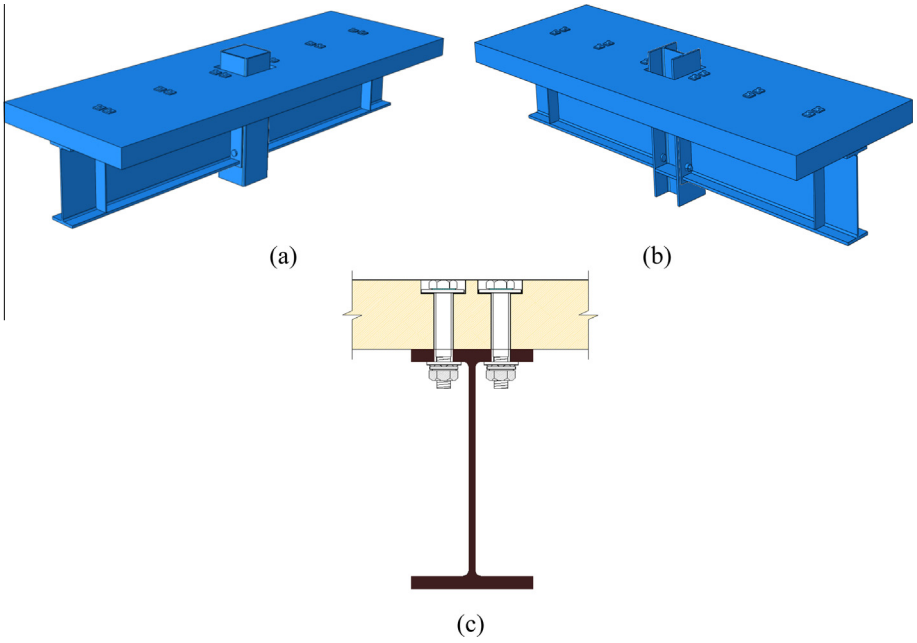

Fig. 1. Schematic outline of deconstructable composite beam-to-column joint with flush end plate connection: (a) pictorial view of CJ1 and CJ2; (b) pictorial view of CJ3 and CJ4; and (c) bolted shear connection.

Table 1
Test specimen.

Specimen	Column type	Steel beam	Shear connector	Degree of shear connection (%)	Hole diameter in slab (mm)	Hole diameter in steel beam (mm)	Applied bolt pretension (kN)
CJ1	250 × 250 × 12.5 mm	460UB82.1	6M20	195	24	22	145
CJ2	250 × 250 × 12.5 mm	460UB82.1	6M16	124	20	18	95
CJ3	250UC89.5	460UB82.1	4M16	82	20	18	95
CJ4	250UC89.5	460UB82.1	4M20	130	24	22	145

All four cruciform joints (*viz.* CJ1–CJ4) comprised of 460UB82.1 steel beam sections. For specimens CJ1 and CJ2, the columns were concrete-filled tubular steel columns having 250 × 250 × 12.5 mm dimensions and for specimens CJ3 and CJ4, 250UC89.5 I-section steel columns of were used. Composite action between the precast concrete slabs and steel beams was provided by the bolted shear connectors installed in pairs as shown in Fig. 1. Grade 8.8 M20 or M16 high strength bolts were used to attach the precast concrete slab to the top flange of the steel beam. The bolted shear connectors were installed from the top and the nuts were tightened from below as shown in Fig. 1. In order to confirm the minimum post-tensioning forces of 95 kN and 145 kN induced in the M16 and M20 bolts respectively, an electric control torque wrench with Squirter Direct Tension Indicating (SDTI) washers were used. The outline and general configuration of the cruciform joints before installation of the precast concrete slabs is shown in Fig. 4, and the precast concrete slabs after de-moulding is shown in Fig. 5.

According to the provisions of EC3 and EC4, in order to prevent non-ductile failure of connections made up of mild steel grades, the thickness of the end plate should be limited to 60% of the bolt diameter (*e.g.* 12 mm thick plate for M20 bolts and 15 mm thick plate for M24 bolts). However, in a study conducted by Ataei et al. [21], it was shown that the end plate thickness recommended in EC3/EC4 cannot sufficiently prevent the non-ductile mode of failure associated with rupture of the bolts in FEPSR beam-to-column composite joints with deconstructable PFBSCs, mainly because of the stiffening effect of reinforced concrete slabs that has not been considered in the EC3/EC4 recommended end plate thickness. Because of this, an 8 mm thick flush end plate (40% of the M20 bolt diameter for the concrete-filled column and about 35% of the M24 bolt diameter for the I-section column) made of S690 grade steel was welded to the end of the steel girders to ensure a ductile mode of failure. Six Grade 8.8 M20 Hollow-bolts (blind bolts) [28] and four M24 Grade 12.9 bolts [29] were used for connecting the steel girders to the CFST columns and I-section columns, respectively.

In all joints tested, the precast GC concrete slabs attached to the top flange of the steel girders were continuous over the column as shown in Fig. 6. The main intention in this experimental study was to determine the influence of one layer of reinforcing steel bars in the steel–concrete composite beam-to-column sub-assemblages. However, the push-out test results [17,22] had shown that in lightly reinforced concrete slabs, severe concrete cracking may take place around the bolted shear connectors, owing to stress concentrations. Accordingly, two layers of reinforcing bars were placed in the slab to prevent cracking of the slabs around the bolted connectors and one layer (the bottom layer) was curtailed near the face of column to provide a longitudinal reinforcing ratio of 0.73% with the reinforcing bar configurations shown in Figs. 2 and 3. Moreover, two layers of N10 bars were used in the transverse direction (Figs. 2 and 3) to prevent the longitudinal splitting of the precast slabs. The configuration of specimens CJ1 and CJ2 after assembling the continuous precast concrete slab are shown in Fig. 6. It is noteworthy that increasing the amount of longitudinal reinforcing bars can increase the peak load capacity and reduce the rotational capacity of composite beam-to-column joints as demonstrated by the finite element simulations [22].

Since installation of the precast concrete slab can be difficult when the columns are high above the floor level, an alternative deconstructable system can be used, in which the precast concrete slabs are not continuous and the flexural resistance against negative bending moment is provided by post-installed steel bars, as described in [21,22].

2.2. Instrumentation

Strain gauges, inclinometers and Linear Strain Conversion Transducers (LSCTs) were employed to respectively measure the strains, rotations and displacements at different locations within the specimens and to assess the structural performance and behaviour of deconstructable beam-to-column joints with a HSS end plate and composite beams. In order to measure the deformation of the end plates and the vertical deflection at the end of the steel beams and also to characterise the relative slip between the precast concrete slab and the steel girder, ten LSCTs were used. In addition, the rotation of the steel beams and column was measured using four electronic inclinometers having an accuracy of 0.01 degrees. The location of the LSCTs and inclinometers are shown in Fig. 7.

A total of twenty-nine YEFCA-5 strain gauges having a maximum strain of 10–15% were employed to measure the strains at different locations along the steel beams and columns, as well as the reinforcing steel bars (Fig. 8). Two of the strain gauges (Nos. 10 and 11) were mounted on the transverse bars at the end of the slab and behind the last row of the bolted shear connectors, to measure the splitting tensile strains that develop in the slab (Fig. 8a).

2.3. Experimental setup and loading procedure

The test setup and loading procedure for the composite beam-to-column joints are illustrated in Fig. 9. A vertical displacement-controlled loading was applied to the both ends of the composite beams by a 5 MN capacity actuator and a spreader beam. In order to verify the test setup and performance of the components and instrumentation, before conducting each test, a small load of about 10% of the predicted ultimate load capacity of the specimens was applied to the specimens. Following this, the specimens were unloaded and reloaded, and the deformation was increased monotonically until no further loading could be sustained by the specimen (defined as failure of the specimens). During the loading regime, three displacement rates, *i.e.* 0.3, 0.6 and 1.2 mm/min were used sequentially and application of the displacements was stopped when the load started to fall significantly.

2.4. Mechanical properties of materials

The results of compression and indirect tension tests on concrete cylinders are summarised in Table 2. Uniaxial tension tests were conducted on the high-strength bolted shear connectors, blind bolts, high-strength bolts and N10 and N16 reinforcing steel bars and the results are provided in Table 3. Furthermore, uniaxial tension tests were carried out on coupons taken from the flush end plate made up of HSS S690, the square steel tube, the flange and web of the steel beams and columns and the results are given in

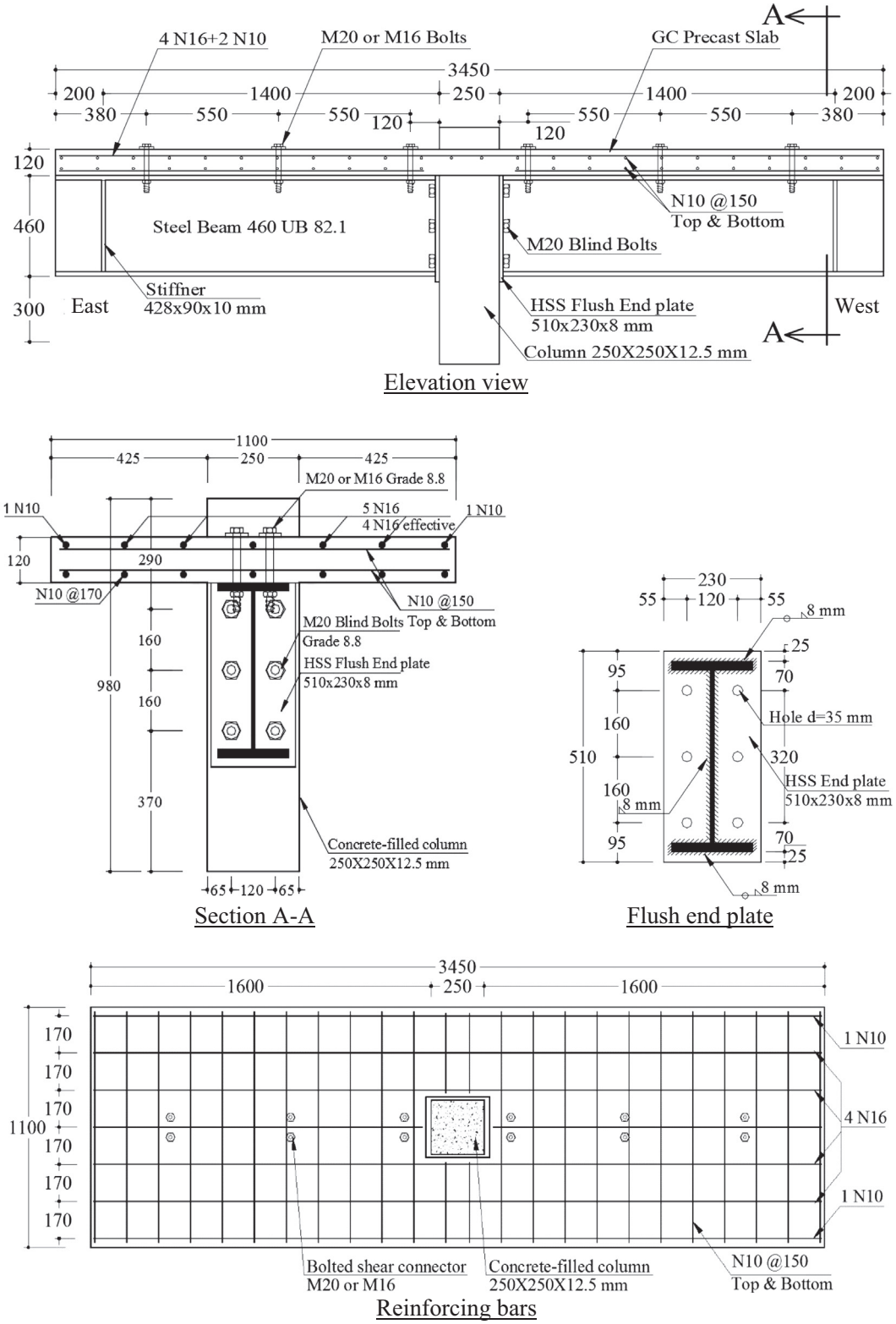

Fig. 2. Geometry and details of joints CJ1 and CJ2 (unit: mm).

Table 3. The stress–strain curve obtained from the uniaxial tension tests on the steel components are shown in Fig. 10. Standard push-out tests on deconstructable composite beams with precast GC concrete slabs and PFBSCs were carried out [20] to characterise the load–slip behaviour and ultimate capacity of the PFBSCs. The key points for characterising the load–slip behaviour of the PFBSCs were derived from the push-out tests results and given in Table 4 [20].

3. Experimental results

3.1. Crack pattern and failure mode

A summary of the experimental results for the FEPSR joints tested in this study is given in Table 5. In general, all four specimens, revealed reasonable rotation and moment capacities in

accordance with the requirements of EC3 and EC4. All specimens failed due to fracture of the longitudinal reinforcing bar and fracture of the joint occurred when substantial rotational deformation developed in the connection. A typical failure mode of the specimens is shown in Fig. 11, whilst Fig. 12 illustrates the state of all specimens after the test. The test results also showed that the HSS flash end plates experience large permanent deformations as shown in Fig. 13.

At sections adjacent to the columns and at a load between 70 and 100 kN, the first crack on the top surface of the precast concrete slabs started to develop. The typical pattern of cracks which were mostly concentrated around the perimeter of the column zone is shown in Fig. 14. During the tests, it was observed that increases in the crack width were associated with a decrease in the initial stiffness of the composite joint and a dramatic increase in the tensile strain of the longitudinal reinforcing steel bars.

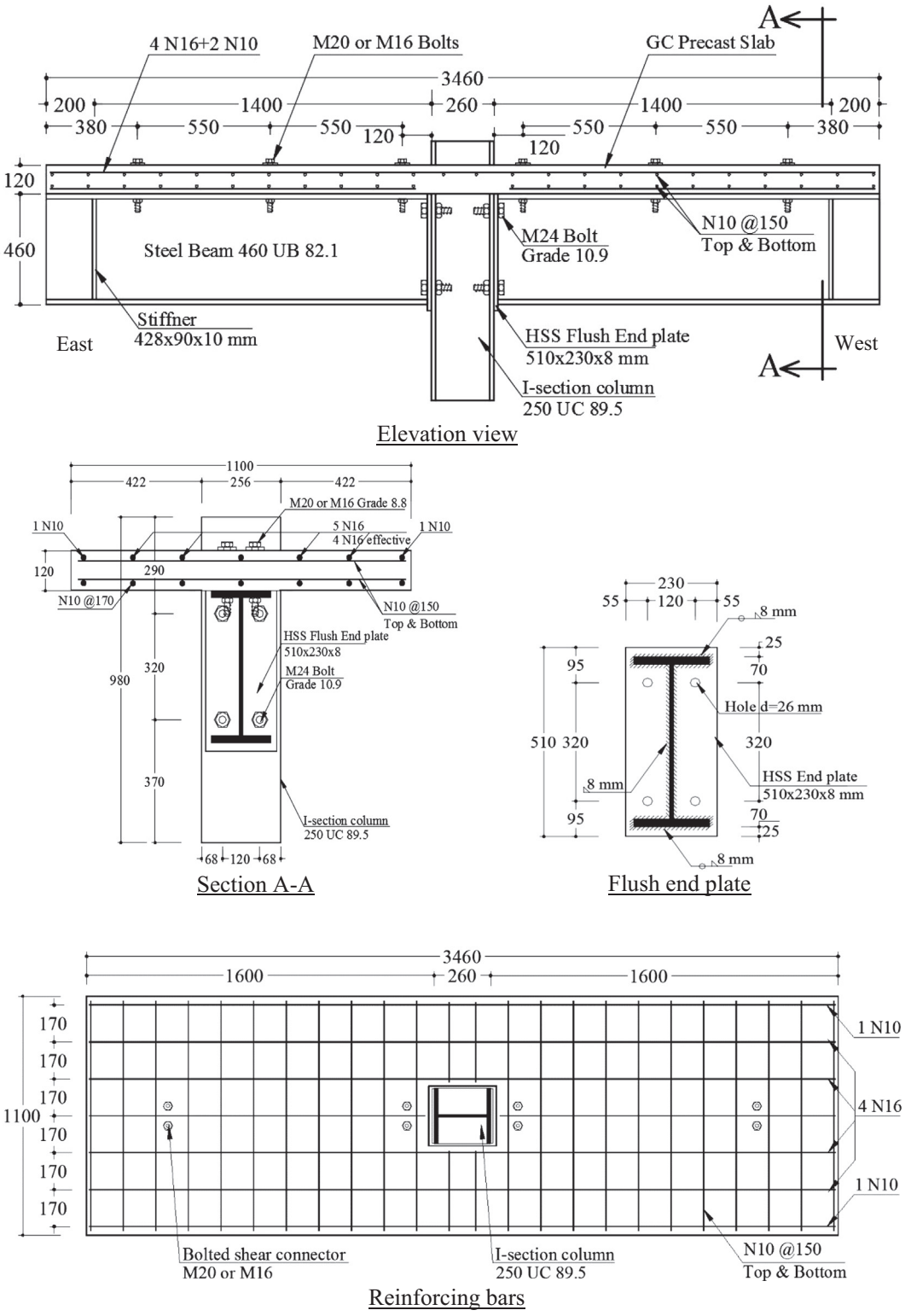

Fig. 3. Geometry and details of joints CJ3 and CJ4 (unit: mm).

Fig. 4. Assembled cruciform steel joints.

Fig. 5. Precast concrete slabs after demoulding.

Fig. 6. Specimens CJ1 and CJ2 ready to be tested.

3.2. Moment–rotation response

The moment–rotation response is a good representative of the behaviour of moment-resisting connections and the moment–rotation response of the beam-to-column joints can be typically characterised by three main parameters; being the initial stiffness, rotation capacity and moment capacity. When HSS materials are used in a connection, the ductility and rotation capacities of the connection should be assessed to ensure that a minimum required ductility and rotation capacity comparable to that of mild steel connections can be provided.

To establish the moment–rotation response of the joints, the moment acting on the connection was obtained by multiplying the load applied at the end of the composite beam by the lever arm (*i.e.* distance between the centre of the loading on the composite beam and the column face). Two different methods were adopted in regard to measuring the rotation of the joints; in the first method, the difference between the rotation of the column and the steel beam measured by inclinometers was considered as the rotation of the connection, whilst in the second method, the rotation of the joint was obtained by subtracting the displacements measured by the bottom LSCT from that measured by the top LSCT (see Fig. 7) and dividing the result by the distance between these two LSCTs. The moment–rotation responses of all four specimens are shown in Fig. 15. Moment capacities of 513, 507, 535 and 535 kN m with rotation capacities of 49, 43, 47 and 44 mrad were observed for specimens CJ1, CJ2, CJ3 and CJ4 respectively, and all specimens exhibited significant non-linearity with very satisfactory moment–rotation behaviour.

According to the provisions of EC3 and EC4, among three possible modes of failure including yielding of the end plate or column flange, bolt failure combined with column flange or end plate yielding and bolt failure, only the first failure mode associated with complete yielding of the end plate or column flange can be considered as ductile and the third mode of failure in which only bolt rupture occurs should be considered as brittle (non-ductile). In the present experimental study, yielding and plastic deformation of the HSS Grade S690 flush end plate in the beam-to-column joints with deconstructable PFBSCs took place with no fracture in the bolts located in the tension zone of the connection, which is a characteristic of the ductile failure mode specified in EC3/EC4. Moreover, in accordance with the EC3 and EC4 provisions, in order to allow for plastic analysis and design, the rotation capacity of the joint must be greater than 30 mrad, and as can be seen in Table 5 all specimens had a rotation capacity higher than that specified in EC3 and EC4. Accordingly, it can be concluded that despite using HSS flush end plates, the proposed deconstructable connections have sufficient rotation capacity and can be considered as ductile.

3.3. Strain in longitudinal reinforcing bars

The load versus tensile strain in the longitudinal reinforcing bars at the mid-span of all specimens is shown in Fig. 16. The sudden increase in the tensile strain in the steel bars at a load of about 80 kN can be attributed to the development of transverse crack in the precast concrete slab and at sections adjacent to the column. Moreover, it was observed that the average strain in the longitudinal reinforcing bars at mid-span for all composite specimens, including the ones with weak partial shear interaction (*i.e.* specimen CJ3), exceeded the yield strain at the ultimate load. The length over which reinforcing bars had yielded has a significant effect on the rotation capacity of the composite joint. Accordingly, the tensile strain in the reinforcing steel bars at different load levels and locations along the composite beams were measured and the results are shown in Fig. 17. It can be seen that the longitudinal reinforcement yielded over a length of 400 mm away from the face of the column. This length is about 0.9 that of the steel beam depth and out of this plastic zone, the strain in the reinforcing bars is very small and remains well below the yield strain of the steel.

3.4. Strain in transverse reinforcing bars

The load versus tensile strain response in the transverse steel reinforcement at the section 1400 mm away from the column face as measured by strain gauges 10 and 11 (Fig. 7) is shown in Fig. 18. It can be seen that the tensile strain in the top and bottom transverse bars is very small and remains within the elastic range. The

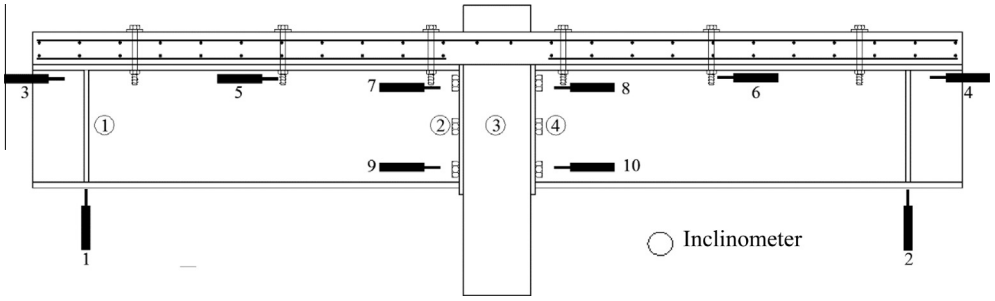

Fig. 7. Layout of LSCTs and inclinometers mounted on steel beams and column.

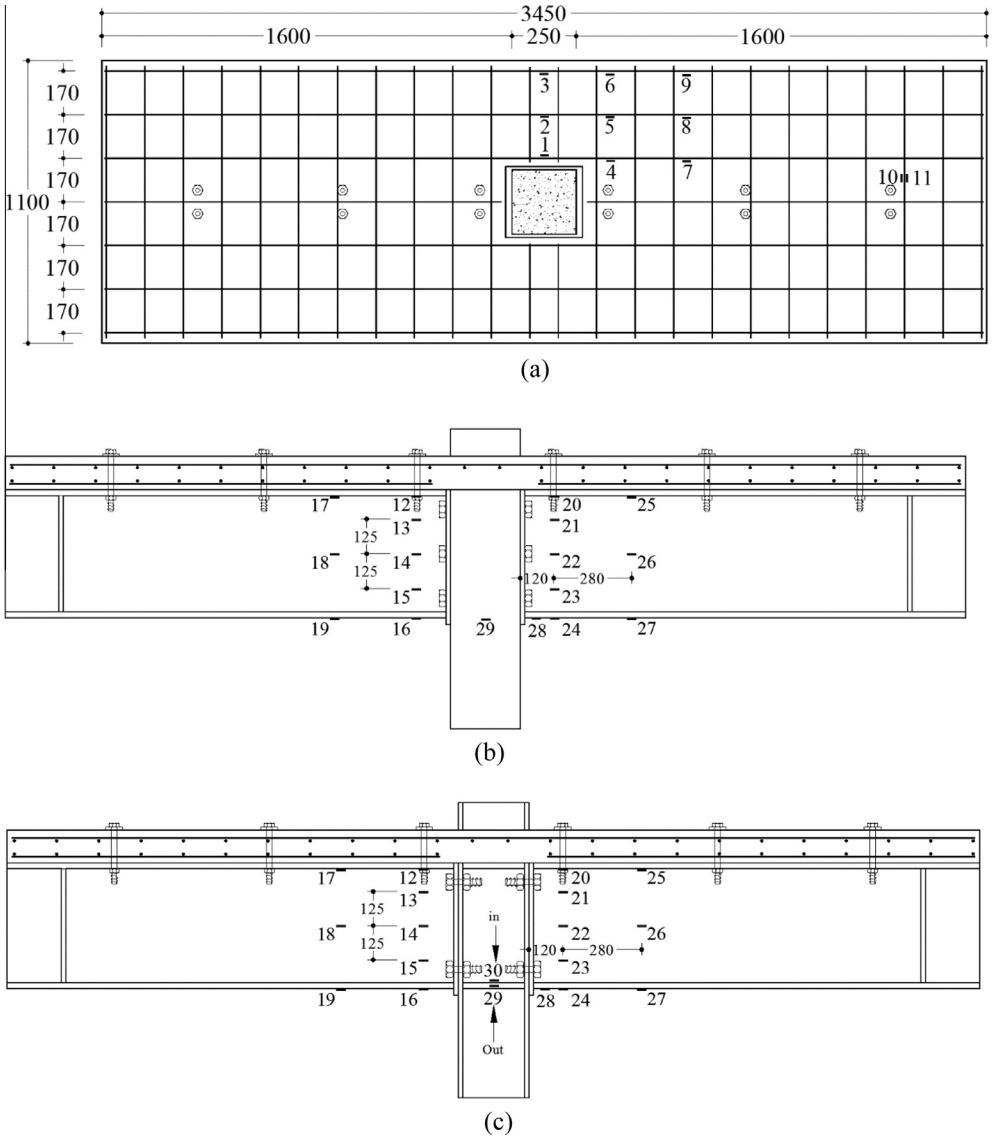

Fig. 8. Layout of strain gauges (a) on reinforcing bars for all specimens and on steel beams and column, (b) for CJ1 and CJ2 and (c) for CJ3 and CJ4.

maximum strain in the transverse bars was about 1030 microstrain.

3.5. Strain in flanges of steel girders

The load versus strain (along the beam axis) response in the top and bottom flanges of the steel girder at sections 120 mm and 400 mm away from the column face is shown in Fig. 19. It can be seen that the compressive strain in the bottom flange of the steel beam is higher than the tensile strains in the top flange, owing to the contribution of the reinforced concrete slab in resisting tensile flexural stresses. In Fig. 19, negative and positive values denote compressive and tensile strains respectively. It is observable that the bottom flange of the steel beam experiences higher absolute strains than the top flange, and hence the neutral axis of the steel beam is located above the centroid of the steel beam. Also, it can be

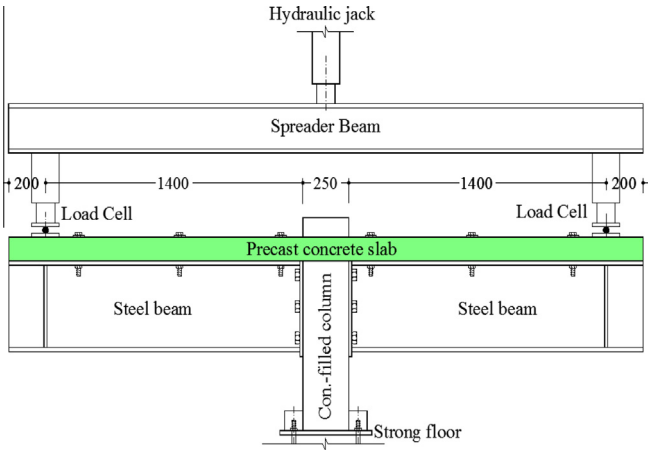

Fig. 9. Test set up for the joint tests.

seen that the tensile and compressive strains in the flanges of the steel beams for all specimens remains within the elastic range during the test. Accordingly, the load carrying capacity of the steel beams can be exploited by providing more reinforcing bars in the slabs, provided local buckling in the bottom (compressive) flange of the steel beam is effectively prevented. The load versus strain response of the bottom flange of the steel girder at the section adjacent to the column face (50 mm away from the column face) was also measured by strain gauge 28 (Fig. 8) during the tests and the results are shown in Fig. 20. It is seen that in this highly plastic zone, the compressive strains in the bottom flange of the steel beam have exceeded the yield strain at the ultimate stages of loading.

3.6. Strains in the columns

The horizontal strain in the stiffeners located at the same level as the bottom flange of the steel beam and in the outer surface of the CFST column at the location of the bottom flange of the beam was measured for the I-section columns by strain gauges 29 and 30 (Fig. 8) and for the CFST columns by strain gauge 29 (Fig. 8) respectively, and the results are shown in Fig. 21.

It is seen that the level of the strain in the steel tube is much lower than that in the stiffeners of the I-section columns. In other words, although the compressive force transferred from the bottom flange of the steel beam to the CFST column is very large, the strain in the steel tube is very small (much lower than the yield strength), owing to the beneficial effect of the concrete in the steel tube. Moreover, yielding or local buckling was not observed in the columns (neither in the I-section nor in the CFST) and stiffeners.

3.7. Bolted shear connectors

The load versus slip relationships at the middle and at the free ends of the composite beams for all specimens are shown in Fig. 22, and the maximum slip for each of the specimens obtained from the tests is given in Table 6. It is observed that the maximum slip at the middle and free ends of the beam increases as the degree of shear connection decreases. The maximum end slip at the precast concrete slab and steel beam interface is 1.72 mm, 3.10 mm, 4.50 mm and 3.12 mm for CJ1, CJ2, CJ3 and CJ4 respectively. The final slip between the steel beam and precast concrete slab for specimen CJ3 which has the lowest degree of composite shear interaction is about 5.5 mm and 4.5 mm at the middle and the free end of the composite beams respectively. In contrast, these parameters for CJ1 which has the highest degree of shear connection are 1.9 mm and 1.7 mm at the middle and the free end of the composite beams respectively. In the first stage of loading where full-composite action is achieved by the friction-grip mechanism of the bolted shear connectors, the slip is almost zero and the first slip takes place at a load of around 200 kN, 160 kN, 160 kN, and 190 kN for specimens CJ1 to CJ4 respectively, and then the slips gradually increase up to the ultimate load with no sudden slip between the precast concrete slab and the steel beam within the loading stage. With regard to the load–slip responses shown in Fig. 22, it can be concluded that first slip in the stronger bolted shear connectors takes place at higher levels of load, and partial shear connection leads to more ductile load–slip behaviour for the composite joint (Fig. 22).

With regard to the relationship between the initial stiffness of the composite joint and the degree of shear connection, it can be seen from the test results that decreasing the degree of shear connection leads to a decrease in the initial strength of composite joint (Table 5) that in turn can increase the deflection of the composite beam under service-load conditions.

In traditional composite joint tests (with a cast *in-situ* concrete slab and welded stud connectors) conducted by Loh et al. [30], Anderson and Najafi [31], Brown and Anderson [32] and Lam and Fu [33], the maximum slip with full shear action was almost zero and hence insignificant. In contrast, the maximum slip for composite joints with deconstructable PFBSCs even for composite joints with full shear connection was not zero due to the oversized holes and the clearance between the bolt shank and bolt holes in the precast concrete slab as well as the clearance between the bolt shank and bolt holes in the top flange of steel beam. From the

Table 3
Mechanical properties of reinforcing steel bars, steel column and beams, flush end plate, bolted shear connectors and bolts.

Specimen	Yield strength (MPa)	Ultimate strength (MPa)	Young's modulus (GPa)
Steel beam flange	348.2	521.5	200
Steel beam web	389.2	556.3	217
Steel column web	351.5	522.8	202
Steel column flange	328.7	524.7	192
Square steel tube	295.1	425.2	200
HSS flush end plate	817.7	832.1	202
Bolted shear connector	837.1	926.3	226
N10 bar	610.1	790.2	200
N16 bar	535.1	631.1	200
Blind bolt	890.2	980.6	199

Table 2
Compressive and indirect tensile strength of concrete.

Specimen	Compressive strength (MPa)					Tensile strength (MPa)		Young's modulus (MPa)
	7 days	14 days	21 days	28 days	Testing days	28 days	Testing days	Testing days
CJ1	35.6	38.5	39.3	39.8	48.8	4.43	4.75	32,470
CJ2					48.1		4.60	
CJ3					48.9		4.78	
CJ4					49.1		4.81	

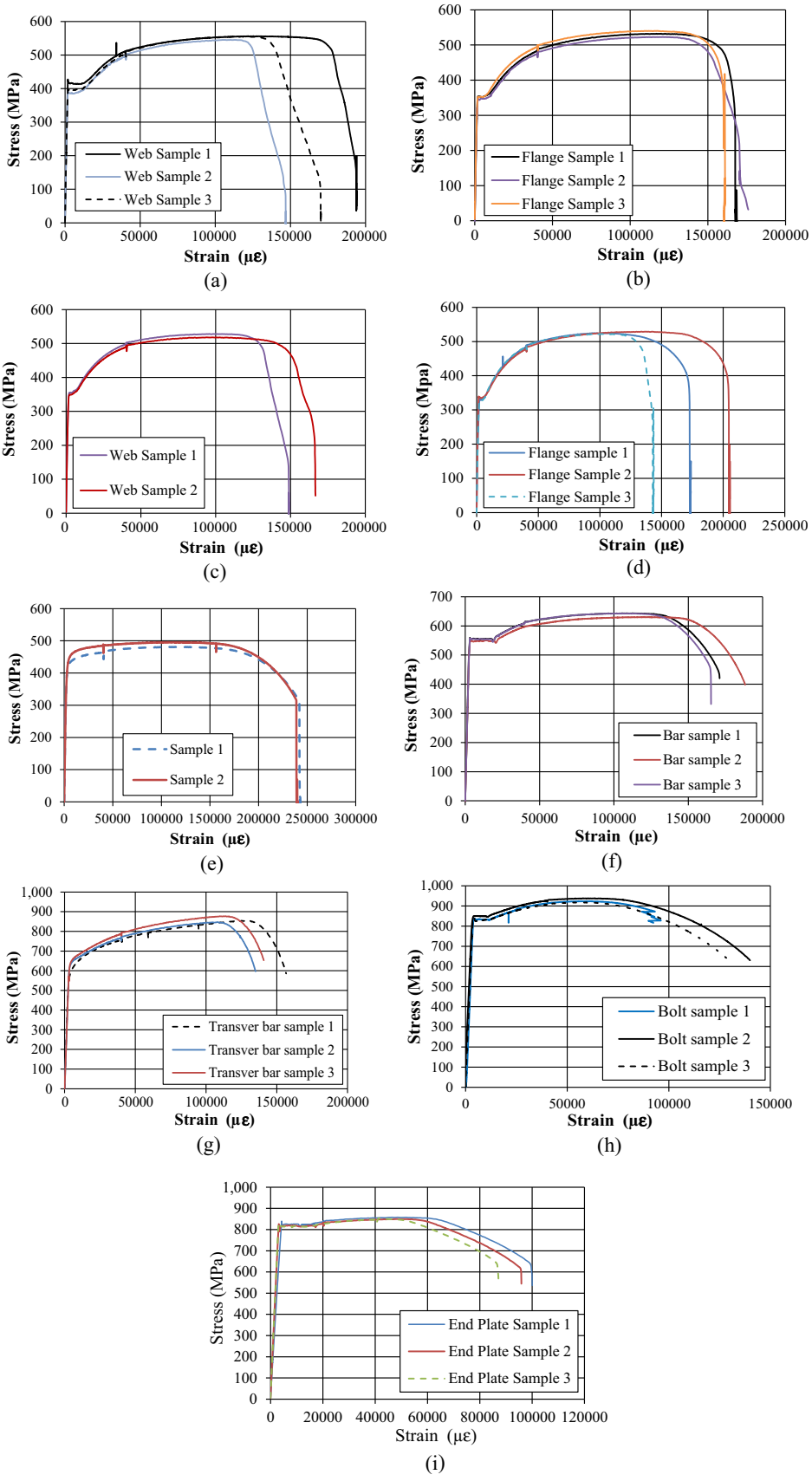

Fig. 10. Stress–strain response (a) beam web, (b) beam flange, (c) column web, (d) column flange, (e) tubular column, (f) longitudinal bars, (g) transverse bars, (h) HSS bolts, and (i) HSS end plate.

Table 4
Summary of push-out test results on PFBSCs.

Shear connector	P_f (kN)	P_u (kN)	S_a (mm)	S_{au} (mm)
M16	36	127	3	12.80
M20	48	201	3	14.93

Notes: P_f = load per bolt for first slip; P_u = ultimate load per bolt; S_a = average slip at first bearing; and S_{au} = average slip at ultimate load.

Table 5
Test results of FEPSR beam-to-column composite joints.

Specimen	Moment capacity (kN m)	Rotation capacity (mrad)	Initial stiffness (kN m/mrad)	Mode of failure
CJ1	513	48	103	Bar fracture
CJ2	507	43	84	Bar fracture
CJ3	535	47	76	Bar fracture
CJ4	535	44	101	Bar fracture

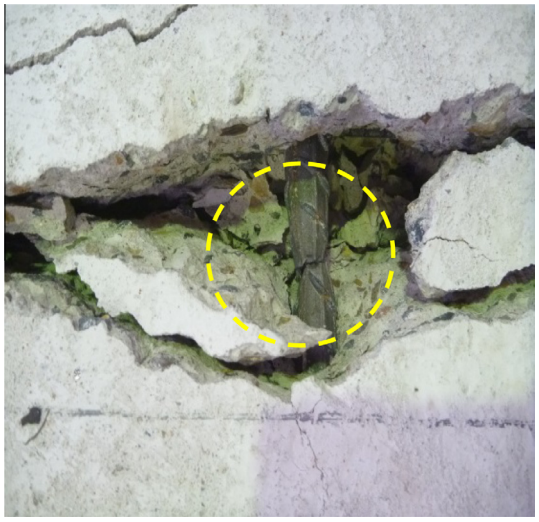

Fig. 11. Typical failure mode of the specimens associated with rupture of reinforcing bars.

experimental results, it can be concluded that composite joints with deconstructable PFBSCs experience a minimum slip which is equal to the sum of the clearances between the bolt shank and bolt holes in the precast slab and between the bolt shank and bolt hole in the top flange of steel beam.

3.8. Deconstructability of the system

One of the main objectives of this study was to propose a novel system that can be easily deconstructed at the end of the service life of the structure, and to facilitate possible recycling and reuse of the steel and concrete components. Therefore, in addition to the structural performance assessment of the composite beam-to-column joints, the deconstructability of the system was also evaluated. To verify that the proposed system can be easily deconstructed, specimen CJ4 was loaded up to 40% of the predicted ultimate load capacity (about the maximum service load level), and then the specimen was unloaded. The specimen was removed from the testing rig and the composite beams were dismantled and then reassembled as shown in Fig. 23. The specimens were then reloaded until failure occurred. This demonstrated that the FEPSR beam-to-column composite joints with PFBSCs can be demounted easily at the end of their service life, and all components of this system can be pulled apart and reused in other buildings. Moreover, one of the blind bolts employed in the concrete-filled steel tube (CFST) column of specimen CJ2 was untightened and removed from the connection and then retightened (Fig. 24), to demonstrate the possibility for deconstruction of blind bolted FEPSR connections at the end of their service life. The use of CFST columns in real structures can hinder the possibility of having fully prefabricated or fully deconstructable structures, mainly because the steel tube columns are filled with concrete on the construction site and such CFST column cannot be recycled easily. However, the proposed system still allows for easy dismantling of a large part of the structures including the concrete slabs as well as steel girders connected to CFST column through blind bolted flush end plates. However, the columns in practice would have some form of splicing by bolting that would allow for the possible use of the column sub-assemblies after deconstruction.

4. Analytical model

A simple model based on the rigid plastic analysis concept is proposed here [21] to determine the main parameters, including the initial stiffness, the moment capacity and the rotation capacity for FEPSR beam-to-column joints with PFBSCs.

4.1. Moment capacity

A component-based modelling approach proposed by EC3 and EC4 is used to calculate the moment capacity of the joints [21]. According to this procedure, the moment capacity of FEPSR beam-to-column joints with PFBSCs can be obtained from

$$M_j = F_r(h_{bm} + h_s - 0.5d_{rb} - c_s - 0.5t_{fb}) + F_{bo1}(h_{bm} - 0.5t_{fb} - h_4), \quad (1)$$

if $F_{rb} + F_{bo1} \geqslant F_{bf}$, and from

$$M_j = F_r(h_{bm} + h_s - 0.5d_{rb} - c_s - 0.5t_{fb}) + F_{bo1}(h_{bm} - 0.5t_{fb} - h_4) - 0.5F_{cw}(y_w + t_{fb}), \quad (2)$$

if $F_{rb} + F_{bo1} < F_{bf}$. In Eqs. (1) and (2), F_{rb} is the tensile strength of the longitudinal reinforcing bars, F_{bf} the compressive resistance of the bottom flange of the steel beam, F_{ob1} the tensile force in the bolts at the top row, h_{bm} the depth of the steel beam, h_s the thickness of the precast concrete slab, d_{rb} the diameter of the longitudinal bars, c_s the longitudinal reinforcement cover, t_{tb} the thickness of the beam bottom flange and h_4 the distance between the centroid of the top row of bolts and the top flange of the beam (Fig. 25). Furthermore, F_{cw} denotes the compressive force at the lower part of the beam web and y_w denotes the depth of web under compression, being obtained from

$$y_w = \frac{F_{rb} + F_{bo1} - F_{bf}}{t_w f_{y,w}}, \quad (3)$$

where t_w is the thickness of the beam web and $f_{y,w}$ the yield strength of the web. Due to the small tensile strength of the concrete, the tensile force generated in the concrete slab is ignored in the calculation. In Eqs. (1) and (2), the forces induced in the middle and lower rows of bolts were assumed to be zero and accordingly the contribution of these bolts in the moment capacity of the connection was ignored. Moreover, the contribution of the partial shear interaction on the bending moment capacity of the composite joints

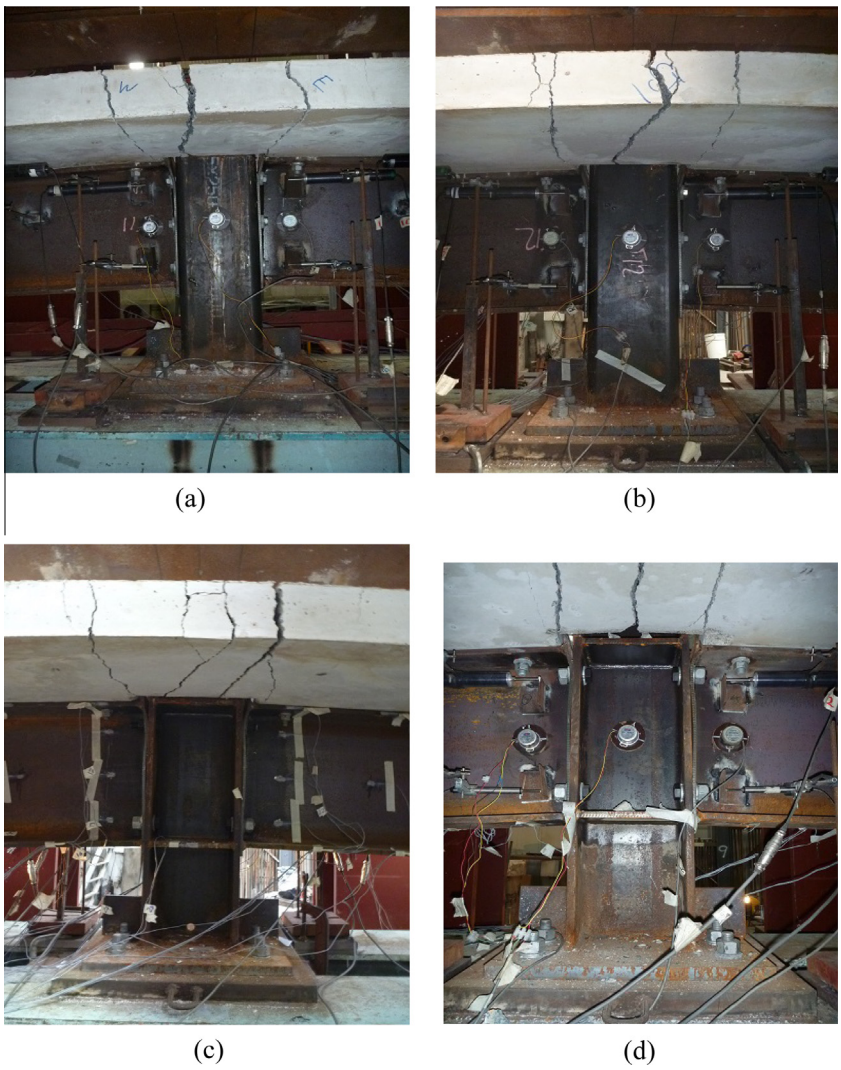

Fig. 12. Specimens after the test (a) CJ1, (b) CJ2, (c) CJ3 and (d) CJ4.

has not been considered in this model. Using the proposed formulae, the moment capacities of the connections were calculated and the results are compared with the test results in Table 7. The results show that the rigid-plastic model adopted can predict the moment capacity of the specimens CJ3 and CJ4 with sufficient accuracy. However, it is observable that the adopted model underestimates (about 14%) the moment capacity of specimens CJ1 and CJ2. This may be attributed to the assumption of zero tensile forces in the middle row of bolt for these two specimens.

4.2. Initial stiffness

The initial stiffness of FEPSR beam-to-column composite joints with PFBSCs can be obtained from the component-based method of EC3 and EC4 [26,27]. In this method, each component of the connection is represented by an elastic spring as shown in Fig. 26. The main components contributing to the initial stiffness of the composite joint are the PFBSCs, the flush end plate, the reinforcing bars, the column walls and the bolts in the connection zone. For the composite joints tested in this study, only the stiffnesses of the flush end plate in bending (k_3), the bolts in tension (k_4), the column flange in bending (k_5), the column web in tension (k_6) and the reinforcing bars in tension (k_7) are considered. It was assumed that the stiffness of the column web in compression (k_1) and the column web in shear (k_2) are infinite due to the use of concrete-filled column and column stiffeners as well as symmetrical loading on the connection. The effective stiffness ($k_{eff,i}$) of the bolt row i (Fig. 25b) can be determined from the equation

$$k_{eff,i} = \left[\frac{1}{k_{3i}} + \frac{1}{k_{4i}} + \frac{1}{k_{5i}} + \frac{1}{k_{6i}}\right]^{-1}. \tag{4}$$

The stiffness of the column web in tension (k_6) for CFST columns (CJ1 and CJ2) was assumed to be infinite due to the use of concrete-filled column. The bending stiffness (k_5) of the flange for concrete-filled tubular columns (*viz.* specimens CJ1 and CJ2) can be determined from

$$k_5 = \frac{\frac{t_{hs}^3}{12(1-\nu^3)}}{\gamma_f (H_o - 2t_{hs})^2}, \tag{5}$$

and for I-section columns (*viz.* specimens CJ3 and CJ4), the bending stiffness (k_5) of the flange can be obtained from

$$k_5 = \frac{0.85 l_{eff,is} t_{hs}^3}{m_{is}^3}, \tag{6}$$

where t_{hs} is the thickness of the hollow-section steel column, ν the Poisson's ratio of steel, H_o the outer dimension of the concrete-filled tubular steel column, $l_{eff,is}$ the smallest of the effective lengths in the

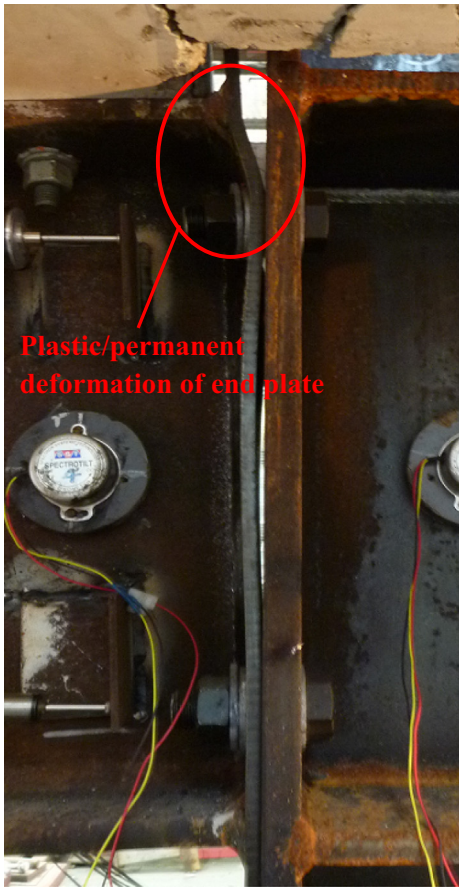

Fig. 13. Plastic deformation of flush end plate of specimen CJ4 after the test.

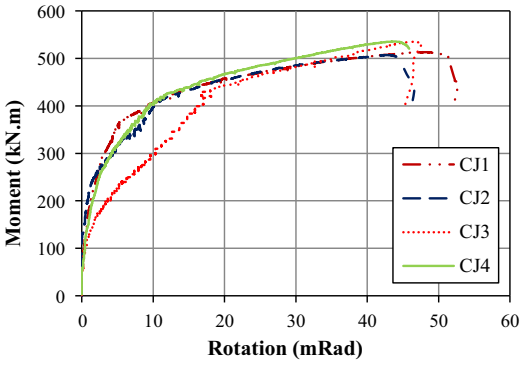

Fig. 15. Moment–rotation response of specimens.

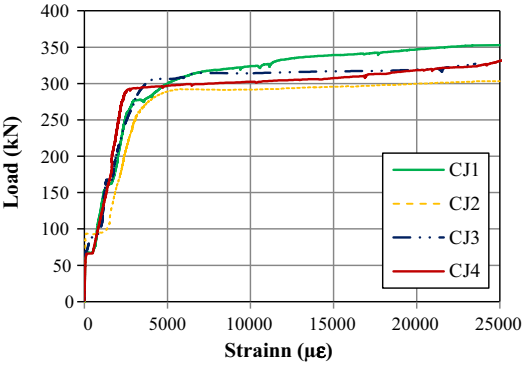

Fig. 16. Tensile strains in longitudinal reinforcing steel bars at mid-span.

I-section steel column flange, m_{is} the distance from the centre of the bolt hole to the start of chamfer on steel column flange and γ_f the deflection coefficient for column flange at bolt location as defined in [34]. The stiffness of the flush end plate in bending (k_3) and the bolts in tension (k_4) can be calculated by equations proposed by Wang et al. [34].

In the adopted procedure, the stiffness of the reinforcing bars (k_7) was combined with $k_{eff,1}$ and $k_{eff,2}$ to form a single equivalent stiffness coefficient (Fig. 26c). The equivalent stiffness can be expressed as

$$k_{eq} = \frac{k_{eff,1}y_1 + k_{eff,2}y_2 + k_7 y_3}{y_{eq}}, \tag{7}$$

where y_{eq} is the equivalent lever arm determine from

$$y_{eq} = \frac{k_{eff,1}y_1^2 + k_{eff,2}y_2^2 + k_7 y_3^2}{k_{eff,1}y_1 + k_{eff,2}y_2 + k_7 y_3}. \tag{8}$$

The initial stiffness of the composite joint can then be written as

$$S_{i,ini} = \frac{E_s y_{eq}}{1/k_{eq}} \quad (\text{in kN mm/mrad}). \tag{9}$$

Fig. 14. Typical pattern of cracks for specimens (a) CJ1 and CJ2 & (b) CJ3 and CJ4.

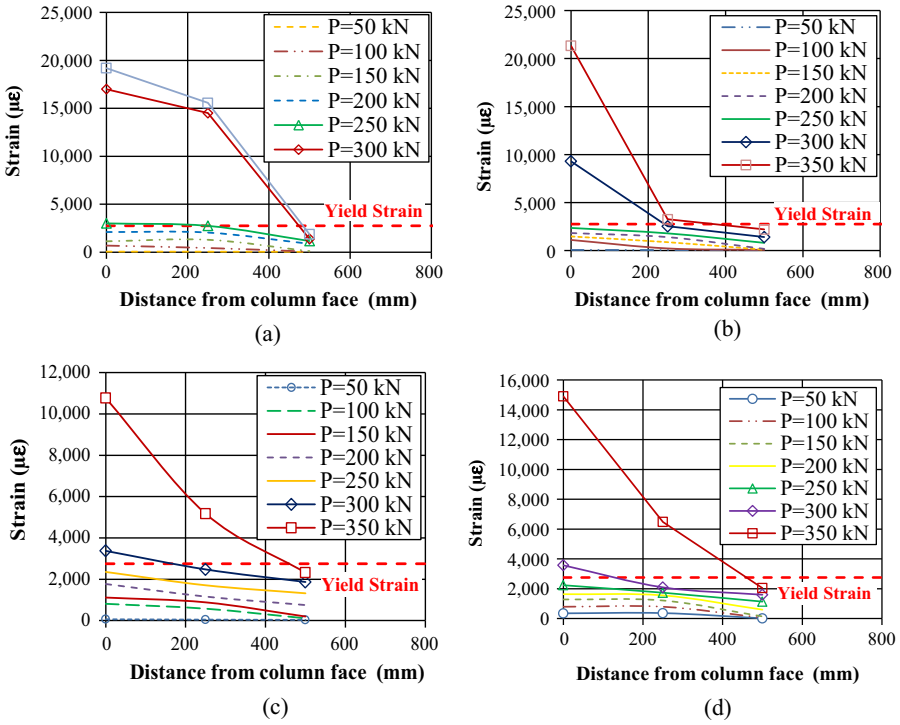

Fig. 17. Tensile strain in reinforcing steel bars at different load levels and locations along the precast slab for specimens (a) CJ1, (b) CJ2, (c) CJ3 and (d) CJ4.

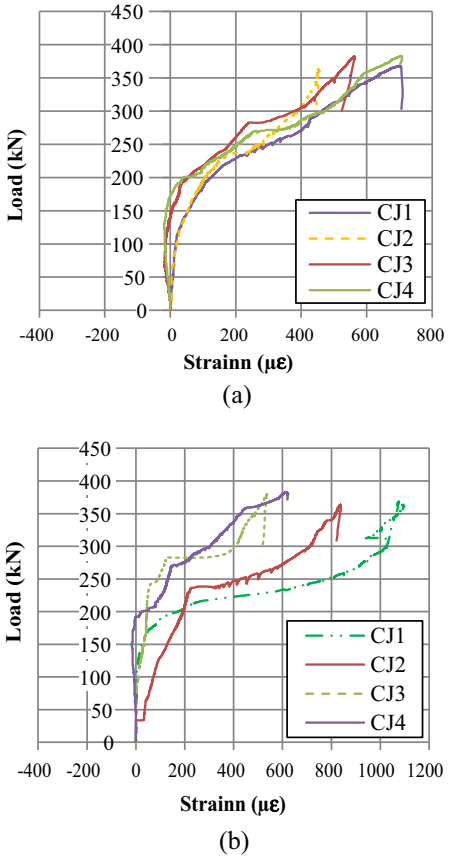

Fig. 18. Load versus tensile strain in transverse steel bars at a section 1400 mm away from the column face (a) top bar and (b) bottom bar.

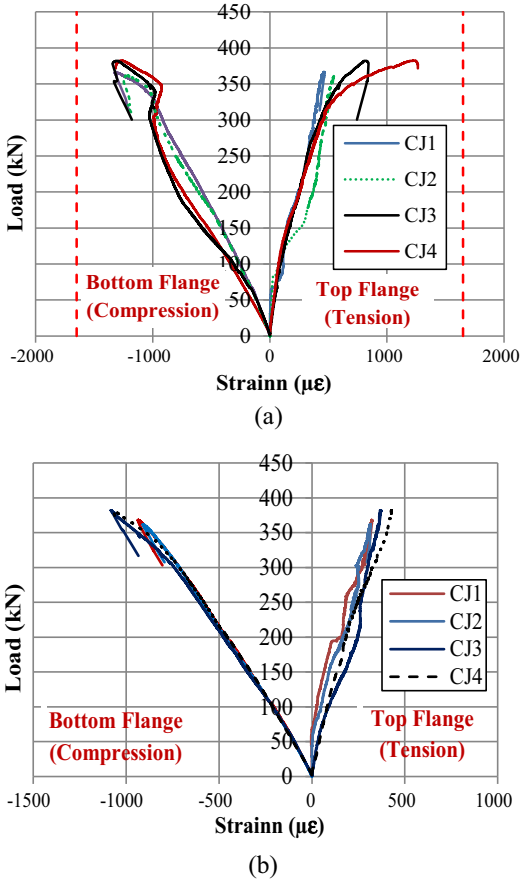

Fig. 19. Load versus strain in bottom and top flange of the steel girder at sections (a) 120 mm and (b) 400 mm away from the column face.

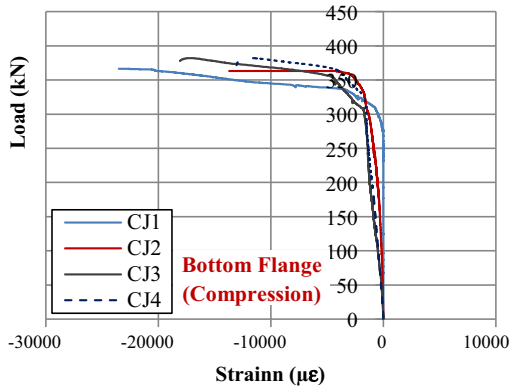

Fig. 20. Load versus strain in bottom flange of the steel girder at sections 50 mm away from the column face.

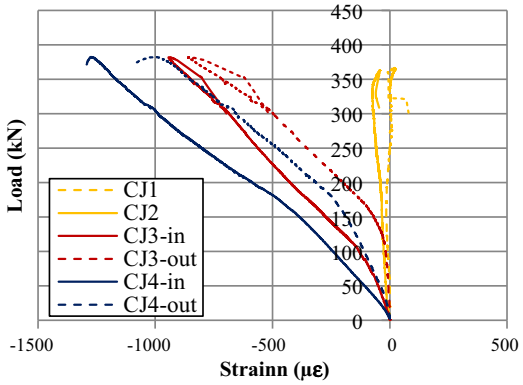

Fig. 21. Load versus strain response on the outer surface of the CFST column (CJ1 and CJ2) and on the bottom column stiffener (CJ3 and CJ4).

Table 6
Summary of load–slip response of specimens.

Specimen	$S_{u,e}$ (mm)	$S_{u,m}$ (mm)	P_e (kN)	P_m (kN)
CJ1	1.72	1.90	200	200
CJ2	3.10	3.56	161	161
CJ3	4.50	5.54	166	104
CJ4	3.12	4.58	185	110

Notes: $S_{u,e}$ = Maximum slip at the end; $S_{u,m}$ = Maximum slip at the end; P_e = load per bolt for first slip at the end; and P_m = load per bolt for first slip at the middle.

Fig. 23. Specimen CJ4 dismantled by untightening and removing the PFBSCs.

A comparison of the connection stiffness predicted by the proposed model and the experimental results is shown in Table 7. It is observable that the adopted model underestimates the initial

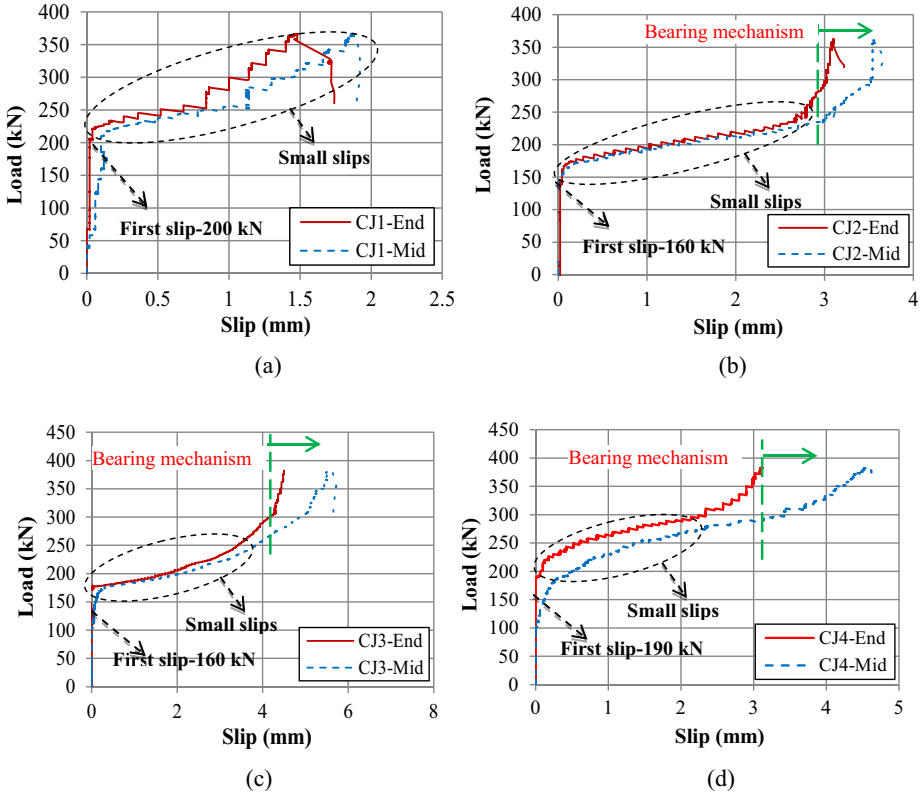

Fig. 22. Load–slip response of the steel–precast concrete composite beams with bolted shear connectors for specimens (a) CJ1, (b) CJ2, (c) CJ3 and (d) CJ4.

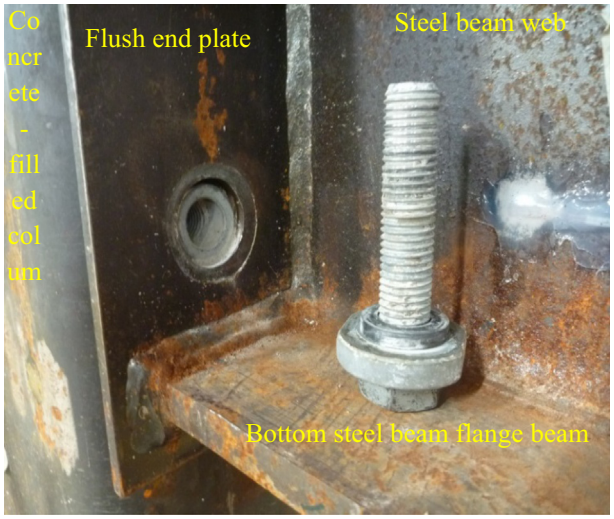

Fig. 24. Deconstructability of the blind bolt connection.

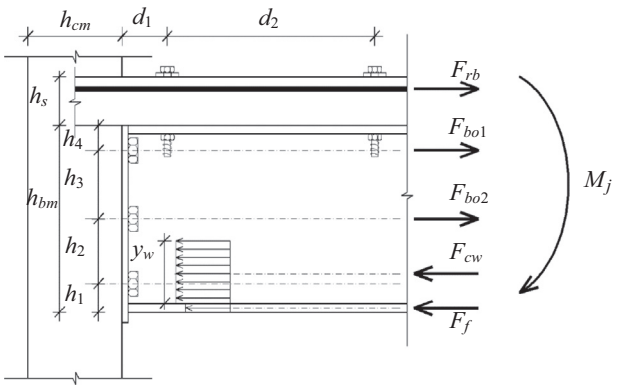

Fig. 25. Schematic outline of geometry and forces acting on composite joint.

Table 7
Comparison of proposed model and test results.

Specimen	M_j (kN m)		$S_{j,ini}$ (kN m/mrad)		θ_j (mrad)	
	Test	Model	Test	Model	Test	Model
CJ1	513	442	103	93	48	41
CJ2	507	442	84	80	43	44
CJ3	535	529	76	64	47	49
CJ4	535	529	101	75	44	45

stiffness of all specimens. The initial stiffness predicted by the model is always conservative and around 5–25% less than the experimental results.

4.3. Rotation capacity

A simple model [21] based on the elongation of the longitudinal bars and the precast concrete slab and the steel beam interface slip is proposed, in which the rotation capacity of the FEPSR beam-to-column joint with PFBSCs can be expressed as

$$\theta_j = \frac{\delta}{h_{bm} + h_s - 0.5d_{rb} - c_s - 0.5t_{fb}} + \frac{s}{h_{bm} - 0.5t_{fb}}, \quad (10)$$

where s is the final slip between the steel beam and precast concrete slab and δ is the elongation of the longitudinal reinforcing bars which can be calculated from

$$\delta = 10\varepsilon_{sy}(d_1 + d_2 + 0.5h_{cm}), \quad (11)$$

where ε_{sy} is the yield strength of bars, l_{sh} the shear span of the composite joint and the definition of other parameters is provided in Fig. 25. The comparison of the rotation capacity predicted by the proposed model and the experimental results is shown in Table 7, which demonstrates reasonable correlation between the model predictions and the experimental results.

5. Conclusions

In this paper, the behaviour of four full-scale sustainable high strength steel Grade S690 FEPSR beam-to-column composite joints with deconstructable PPBSCs was investigated. A novel steel–concrete composite floor with precast concrete slabs associated with low CO_2 emissions during their manufacture, high strength steel, blind bolting and deconstructable Post-installed Friction-grip Bolted Shear Connectors (PFBSCs) was adapted to improve the sustainability of the composite floor and to enhance the possibility for recycling and reuse of construction materials and subsequently to reduce the carbon footprint of the construction industry. The type of bolted shear connectors, degree of shear connection and column type were the main variables in the experimental program. Based on the experimental results, the structural behaviour of the joints in this novel composite system that takes advantage of precast slabs and PFBSCs in conjunction with high-strength steel flush end plates were investigated. With regard to the beam-to-column test results, the following conclusions are drawn about the structural behaviour of these joints.

- The test results confirm that the HSS FEPSR composite joint with PFBSCs can provide a higher rotation capacity (43 mrad and above) than that specified by the EC3 and EC4 codes.

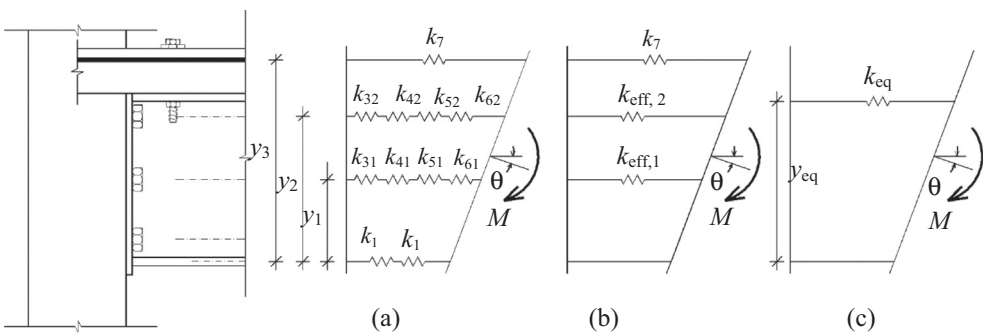

Fig. 26. Initial stiffness model the composite joint.

- A ductile mode of failure (as specified in the provisions of EC3 and EC4) for beam-to-column joints with deconstructable PFBSCs and HSS flush end plates can be achieved, provided the end plate thickness is limited to 35–40% of the bolt size.
- The post-tensioning force induced in the bolted shear connectors can effectively mobilise the friction-grip mechanics and transmit horizontal shear between the precast concrete slabs and the top flange of the steel beam at the early stages of loading. During this early stage, the relative slip between the precast slab and steel beam is negligible. Increasing the size of bolted shear connectors can increase the load corresponding to the first slip in the composite joints.
- Stresses and strains in the steel tube in the lower part of the connection is much lower than that in the I-section column stiffeners, owing to beneficial effect of the concrete infill in the steel tube.
- The general trend for the load–slip response of the composite beam-to-column sub-assemblages with lower degrees of shear connection is similar to that of push-out test results.
- Decreasing the degree of shear connection (composite action) leads to a decrease in the initial strength of a composite joint that in turn can increase the deflection of the composite beam-to-column sub-assemblages under service-load conditions.
- Yielding and plastic deformation of the flush end plate made up of HSS S690 occurred without fracture in the blots located in the tension zone of the connection, provided the thickness of end plate is limited to 35–40% of the bolt size.
- The FEPSR beam-to-column joints with PFBSCs can be deconstructed fairly easily at the end of the service life of the structure, and all components of the proposed system can be pulled apart and reused. Beam-to-column connections using blind bolting can also be deconstructed at the end of the structure's service life.
- Simple component-based models that are adopted in EC4 were proposed. A comparison with the experimental results showed that the models can adequately predict the initial stiffness, rotational capacity and bending moment capacity of the deconstructable HSS beam-to-column joints for design purposes. However, the initial stiffness predicted by the model was always conservative and around 5–25% less than the initial stiffness observed in the test.
- In this study, all specimens had HSS flush end plates and hence the influence of the end plate material strength on the overall joint behaviour could not be assessed solely based on the experimental results provided in this paper. However, a comparison between the test results on composite beam-to-CFST sub-assemblages with mild steel flush end plates [21] and those of this study (with HSS flush end plates) shows that the end plate material has a major effect on the rotation capacity, but its effects on the initial stiffness and moment capacity of the composite joint were found to be insignificant.

Acknowledgements

The work reported in this paper was undertaken with the financial support of the Australian Research Council through an Australian Laureate Fellowship (FL100100063) awarded to the second author. The assistance of the technical staff at the UNSW Heavy Structures Research Laboratory is also acknowledged with thanks.

References

[1] Gogou E. Use of high strength steel grades for economical bridge design. M.S. thesis. Amsterdam: Department of Civil Engineering and Geoscience, Delft University of Technology; 2012.
[2] Mursi M, Uy B. Strength of slender concrete filled high strength steel box columns. J Constr Steel Res 2004;60:1825–48.
[3] Girão Coelho AM, Bijlaard FSK. Experimental behaviour of high strength steel end-plate connections. J Constr Steel Res 2007;63:1228–40.
[4] Girão Coelho AM, Bijlaard FSK, Simões da Silva L. High strength steel in buildings and civil engineering structures: design of connections. Adv Struct Eng Struct 2010;13(3).
[5] Marshall WT, Nelson HM, Banerjee HK. An experimental study of the use of high-strength friction-grip bolts as shear connectors in composite beams. Struct Eng 1971;49:171–8.
[6] Moynihan MC, Allwood JM. Viability and performance of demountable composite connectors. J Constr Steel Res 2014;99:47–56.
[7] Pavlović M, Marković Z, Veljković M, Budevac D. Bolted shear connectors vs. headed studs behaviour in push-out tests. J Constr Steel Res 2013;88:134–49.
[8] Dallam LN. Push out tests with high strength bolt shear connectors. Report for Missouri State Highway Department. Missouri: Department of Civil Engineering, University of Missouri-Columbia; 1968.
[9] Dallam LN, Harpster JL. Composite beam tests with high-strength bolt shear connectors. Report for Missouri State Highway Department. Missouri: Department of Civil Engineering, University of Missouri-Columbia; 1968.
[10] Kwon G, Engelhardt MD, Klinger RE. Behavior of post-installed shear connectors under static and fatigue loading. J Constr Steel Res 2010;66:532–41.
[11] Kwon G, Engelhardt MD, Klinger RE. Experimental behavior of bridge beams retrofitted with post-installed shear connectors. J Bridge Eng ASCE 2011;16:536–45.
[12] Wijesiri Pathirana S, Uy B, Mirza O, Zhu X. Flexural behaviour of composite steel–concrete beams utilising blind bolt shear connectors. Eng Struct 2016;114:181–94.
[13] Bradford MA, Pi Y-L. Numerical modelling of deconstructable composite beams with bolted shear connectors. In: Conference on numerical modeling strategies for sustainable concrete structures, Aix-en-Provence, France, II-2. p. 1–8.
[14] Bradford MA, Pi Y-L. Numerical modelling of composite steel–concrete beams for life-cycle deconstructability. In: 1st International conference on performance-based and life-cycle structural engineering, Hong Kong. p. 102–9.
[15] Bradford MA, Pi Y-L. Nonlinear elastic–plastic analysis of composite members of high-strength steel and geopolymer concrete. Comput Model Eng Sci 2013;2320:1–27.
[16] Rowe M, Bradford MA. Partial shear interaction in deconstructable composite steel–concrete composite beams with bolted shear connectors. In: International conference on design, fabrication and economy of welded structures, Miskolc, Hungary. p. 585–90.
[17] Lee SSM, Bradford MA. Sustainable composite beams with deconstructable shear connectors. In: 5th International conference on structural engineering, mechanics and computation, Cape Town, South Africa.
[18] Ataei A, Bradford MA. FE modelling of sustainable semi-rigid flush end plate composite joints with deconstructable bolted shear connectors. In: International conference on composite construction (CCVII), ASCE, Queensland, Australia.
[19] Ataei A, Bradford MA. Sustainable and deconstructable semi-rigid flush end plate composite joints. In: 1st Australian conference on computational mechanics, Australia, October 2013.
[20] Ataei A, Bradford MA, Liu X. Sustainable composite beams and joints with deconstructable bolted shear connectors. In: 23th Australian conference on the mechanics of structures and materials, Byron Bay, Australia, December 2014.
[21] Ataei A, Bradford MA, Valipour HR. Experimental study of flush end plate beam-to-CFST column composite joints with deconstructable bolted shear connectors. Eng Struct 2015;99:616–30.
[22] Ataei A, A low-carbon deconstructable steel–concrete composite framed system with recyclable beam and slab components. PhD thesis. Sydney, Australia: School of Civil and Environmental Engineering, University of New South Wales; 2016.
[23] Ataei A, Bradford MA, Liu X. Experimental study of composite beams having a precast geopolymer concrete slab and deconstructable bolted shear connectors. Eng Struct 2016;114:1–13.
[24] Ataei A, Bradford MA, Liu X. Experimental study of flush end plate beam-to-column composite joints with precast slabs and deconstructable bolted shear connectors. Structures 2016;7:43–58.
[25] Boral Australia. <http://www.boral.com.au/concrete/pdf/BOR3040-Envisia_Brox_V10 _FINAL _LR.pdf>.
[26] British Standards Institution. Eurocode 3: design of steel structures: Part 1.1. General rules and rules for buildings, BS EN 1993-1-1. London: BSI; 2005.
[27] British Standards Institution. Eurocode 4: design of composite steel and concrete structures: Part 1.1. General rules and rules for buildings, BS EN 1994-1-1. London: BSI; 2006.
[28] Lindapter®. Hollo-Bolt®. <www.ancon.com.au/downloads/s3/l1/hollo-bolt.pdf>.

[29] Standards Australia. AS 1252: high strength steel bolts with associated nuts and washers for structural engineering. SA, Sydney; 1996.
[30] Loh HY, Uy B, Bradford MA. The effects of partial shear connection in composite flush end plate joints. Part I – experimental study. J Constr Steel Res 2006;62:232–46.
[31] Anderson D, Najafi AA. Performance of composite connections: major axis end plate joints. J Constr Steel Res 1994;31:31–57.
[32] Brown ND, Anderson D. Structural properties of composite major axis end plate connections. J Constr Steel Res 2001;57:327–49.
[33] Lam D, Fu F. Experimental study on semi-rigid composite joints with steel beams and precast hollowcore slabs. J Constr Steel Res 2006;62:771–8.
[34] Wang JF, Han LH, Uy B. Behaviour of flush end plate joints to concrete-filled steel tubular columns. J Constr Steel Res 2009;65:925–39.